Automodel Solutions of Non-steady-state Biberman-Holstein Equation for Voigt and Holtsmark Broadening of Spectral Lines

A.B. KUKUSHKIN[1,2,3,] V.S. NEVEROV[1], P.A. SDVIZHENSKII[1], V.V. VOLOSHINOV[4]

[1]*National Research Center "Kurchatov Institute", Moscow, 123182, Russian Federation*

[2]*National Research Nuclear University MEPhI, Moscow, 115409, Russian Federation*

[3]*Moscow Institute Physics and Technology (State University), 141700 Dolgoprudny, Moscow Region, Russia*

[4]*Institute for Information Transmission Problems (Kharkevich Institute) of Russian Academy of Science, 127051 Moscow, Russia*

ABSTRACT: The accuracy of approximate automodel solutions [J. Phys. A: Math. Theor. 2016, 49, 255002] for the Green's function of the non-steady-state Biberman-Holstein equation for the Voigt and Holtsmark broadening of spectral lines is analyzed using the distributed computing. The high accuracy of automodel solutions in a wide range of parameters of the problem is shown.

1. INTRODUCTION

The Stark broadening of spectral lines is known to produce the long-tailed spectral line shapes of atom and ion radiation in plasmas (see e.g. [1-8]). In the broad range of conditions in plasmas and gases, where the complete redistribution (CRD) in photon frequency within the resonance line shape is applicable, the radiative transfer is described by the Biberman-Holstein equation for the density of excited atoms [9, 10] and characterized by the infinite mean-squared displacement of the initial perturbation [11] and, respectively, by the irreducibility of the integral equation, in space variables, to a differential one. This makes the respective radiative transfer a nonlocal (superdiffusive) one [12, 13] (for the deviation from the CRD and the limits of its applicability see, e.g., [14]).

The latter makes the numerical simulation of radiative transfer in resonance spectral lines a formidable task. The simple models based on the domination of the long-free-path flights of the photons were suggested [15] and developed for the quasi-steady-state transport problem, now known as the Escape Probability methods (see [16-18]).

For the time-dependent superdiffusive transport, recently a wide class of non-steady-state superdiffusive transport on a uniform background with a power-law decay, at large distances, of the step-length probability distribution function (PDF) was shown [19] to possess an approximate automodel solution. The solution for the Green's function was constructed using the scaling laws for the propagation front (i.e. time dependence of the relevant-to-superdiffusion average displacement of the carrier) and asymptotic solutions far beyond and far ahead the propagation front. These scaling laws were shown to be determined essentially by the long-free-path carriers (Lévy flights [20-24]). The validity of the suggested automodel solution was proved by its comparison with numerical solutions in the one-dimensional (1D) case of the transport equation with a simple long-tailed PDF with various power-law exponents and in the case of the Biberman-Holstein equation of the 3D resonance radiative transfer for various (Doppler,

Lorentz, Voigt and Holtsmark) spectral line shapes. The analysis of the limits of applicability of the automodel solution in the above-mentioned cases was continued in [25]. The full-scale numerical analysis of the limits of applicability was done in [26], using the massive computations of the exact solution of the transport equation with a simple long-tailed PDF with various power-law exponents. The comparison of these results with automodel solutions has shown high accuracy of automodel solutions in a wide range of space-time variables and enabled us to identify the limits of applicability of automodel solutions.

It is important to note that the success of automodel solutions [19] for a wide class of non-stationary superdiffusive transport was achieved due to identification of the scaling laws in the case of radiative transfer in the Biberman-Holstein model in the papers [15, 11, 27, 28, 12, 13, 19, 29, 30].

Here we extend the approach [26] to the case of the Green's function of the 3D Biberman-Holstein equation for the Voigt and Holtsmark line shapes. The main equations are given in Sec. 2.1, Sec. 3 is devoted to verification of approximate automodel solutions, and conclusions are made in Sec. 4.

2. GREEN'S FUNCTION OF NON-STEADY-STATE BIBERMAN-HOLSTEIN EQUATION FOR VOIGT AND HOLTSMARK LINE SHAPES

2.1. Main Equatious

The Biberman-Holstein equation [9, 10] for radiative transfer in a uniform medium of two-level atoms/ions has been obtained from the system of equations for spatial density of excited atoms, $f(\mathbf{r}, t)$, and spectral intensity of resonance radiation. This system is reduced to a single equation for $f(\mathbf{r}, t)$, which appears to be an integral equation, non-reducible to a differential diffusion-type equation:

$$\frac{\partial f(\mathbf{r}, t)}{\partial t} = \frac{1}{\tau} \int_V G(|\mathbf{r} - \mathbf{r}_1|) f(\mathbf{r}_1, t) dV_1 - \left(\frac{1}{\tau} + \sigma\right) f(\mathbf{r}, t) + q(\mathbf{r}, t), \tag{1}$$

where τ is the lifetime of the excited atomic state with respect to spontaneous radiative decay; σ is the rate of the collisional quenching of excitation; q is the source of excited atoms, different from populating by the absorption of resonant photons (e.g. collisional excitation). The kernel G is determined by the (normalized) emission spectral line shape ε_v and the absorption coeffcient k_v. In homogeneous media, G depends on the distance between the points of emission and absorption of the photon:

$$G(r) = -\frac{1}{4\pi r^2}\frac{dT(r)}{dr}, \quad T(r) = \int\limits_0^\infty \varepsilon_v \exp(-k_v r)\, dv. \tag{2}$$

The analytical solution of equation (1) with a point instant source, $q(\mathbf{r}, t) = \delta(\mathbf{r})\delta(t)$, i.e. the Green's function, was obtained in [11] with the help of the Fourier transform:

$$f(r, t) = -\frac{e^{-t\left(\frac{1}{\tau}+\sigma\right)}}{(2\pi)^2 r}\frac{\partial}{\partial r}\left\{\int\limits_{-\infty}^\infty e^{-ipr}\left[\exp\left\{\frac{t}{\tau}J(p)\right\} - 1\right] dp + 2\pi\delta(r)\right\}, \tag{3}$$

where

$$J(p) = \frac{1}{p}\int\limits_0^\infty \varepsilon_v k_v \arctan\frac{p}{k_v}\, dv. \tag{4}$$

The homogeneity of the medium implies that τ and σ are constants. The latter makes the role of quenching easily accounted for by the time exponent $\exp(-\sigma t)$, so in what follows we omit the account of this process, i.e., in fact, for convenience take $\sigma = 0$. Hereafter we use the dimensionless time, assuming the normalization by τ.

The formulae (3) for $r \neq 0$ may be transformed to take the following form:

$$f(r,t) = \frac{1}{(2\pi)^2 r} \int_{-\infty}^{\infty} p\, sin(pr)\, [exp\{t(J(p) - 1)\} - exp\{-t\}] dp. \tag{5}$$

Let us consider two cases of the resonance radiative transfer in the Biberman-Holstein model, namely the case of the Voigt and Holtsmark spectral line shape.

2.2. Exact solutiou for Voigt spectral liue shape

The line shape ε_v is taken in the form [31]:

$$\varepsilon_y(a) = C'(a) \frac{2\sqrt{\ln 2}}{\Delta v_D} W\big(a, \omega(v)\big), \tag{6}$$

where

$$W(a, \omega) = \int_{-\infty}^{+\infty} \frac{e^{-y^2} dy}{a^2 + (\omega - y)^2}, \tag{7}$$

$$\omega = \frac{2\sqrt{\ln 2}\,(v_0 - v)}{\Delta v_D}, \tag{8}$$

$$a = \frac{\Delta v_L}{\Delta v_D} \sqrt{\ln 2}. \tag{9}$$

Here Δv_D is the width of the Doppler line shape, Δv_L is the width of the Lorentz line shape. The coefficient C' (a) is determined by the normalization condition, $\int_0^{\infty} \varepsilon_y dv = 1$.

The respective absorption coefficient $k_v(a)$ has the form

$$k_v(a) = k_0 \frac{W\big(a, \omega(v)\big)}{W(a, 0)}, \tag{10}$$

$$k_0 = n_0 \pi \lambda^2 \frac{W(a, 0)}{\tau} \frac{g_n}{g_0}, $$

where n_0 is the density of absorbing atoms, λ, the wavelength of a photon, g_i, statistical weight of the i-th level. Using Eq. (3.466.1) in [32], W(a,0) may be expressed in the form

$$W(a, 0) = \int_{-\infty}^{+\infty} \frac{e^{-y^2} dy}{a^2 + y^2} = [1 - erf(a)] \frac{\pi}{a} e^{a^2}, \tag{11}$$

where $erf(x)$ is the error function:

$$erf(x) = \frac{2}{\sqrt{\pi}} \int_0^x e^{-t^2} dt. \tag{12}$$

Let us turn in (5) to dimensionless variables $\rho = k_0 r$ and $P = p/k_0$, $v'' = 2\sqrt{\ln 2}\,(v - v_0)/\Delta v_D$ and use equations (6) and (10) for ε_v and k_v. This gives

$$G(\rho; a) = -k_0^3 \frac{1}{4\pi\rho^2} \frac{dT(\rho; a)}{d\rho},$$ (13)

$$T(\rho; a) \equiv C'(a) \int_{-\infty}^{\infty} W(a, -v'') \exp\left(-\frac{W(a, -v'')}{W(a, 0)}\rho\right) dv'$$ (14)

$$f(\rho, t; a) = k_0^3 \frac{1}{(2\pi)^2 \rho} \int_{-\infty}^{\infty} P \sin(P\rho)\left[\exp\{t(J(P; a) - 1)\} - \exp\{-t\}\right] dP, \rho \neq 0,$$ (15)

$$J(P; a) = \frac{1}{P} \frac{C'(a)}{W(a, 0)} \int_{-\infty}^{\infty} [W(a, -v'')]^2 \arctan\frac{PW(a, 0)}{W(a, -v'')} dv''.$$ (16)

2.3. Exact solutiou for Holtsmark Spectral LLne Shape

For Holtsmark spectral line shape the functions ε_v and k_v, which enter the function $J(p)$, for linear Stark effect may be expressed in the form (cf. [3]):

$$\varepsilon_v = \frac{1}{\Delta v_H} \mathcal{H}\left[\frac{v - v_0}{\Delta v_H}\right], \quad \Delta v_H = C_2 F_0, \quad F_0 = 2.603 e N^{2/3},$$ (17)

$$k_v = k_0 \mathcal{H}\left[\frac{v - v_0}{\Delta v_H}\right],$$ (18)

where N is the density of the perturbing particles, $\mathcal{H}(\beta)$, the Holtsmark function:

$$\mathcal{H}(\beta) = \frac{2}{\pi}\beta \int_0^{\infty} x \sin(\beta x) e^{-x^{3/2}} dx.$$

Turning in (5) to dimensionless variables $\rho = k_0 r$ and $P = p/k_0$, p/k_0, $v' = (v - v_0)/\Delta v_H$ and using (17) and (18) for ε_v and k_v, we obtain

$$f(\rho, t) = -k_0^3 \frac{1}{(2\pi)^2 \rho} \frac{\partial}{\partial\rho} \int_{-\infty}^{\infty} \cos(P\rho)\left[\exp\{t(J(P) - 1)\} - \exp\{-t\}\right] dP, \quad \rho \neq 0,$$ (19)

$$J(P) = \frac{1}{P} \int_{-\infty}^{\infty} [\mathcal{H}(v')]^2 \arctan\frac{P}{\mathcal{H}(v')} dv'.$$ (20)

3. APPROXIMATE AUTOMODEL SOLUTIONS AND VERIFICATION OF ACCURACY

3.1. Geueral Equatlous

The approximate automodel solution [19] has the form:

$$f_{\text{auto}}(r,t) = tG\left(rg\left(\frac{r_{\text{fr}}(t)}{r}\right)\right),$$

(21)

where G is the kernel of the Biberman-Holstein equation, g is an unknown function with the following asymptotics:

$$g(s){=}1, s \ll 1,$$

(22)

$$g(s) \propto s, s \gg 1.$$

(23)

For the propagation front, $\rho_{\text{fr}}(t)$, we used in [19, 26] the function which appears to be close to the time dependence of the mean displacement:

$$(t{+}1)T(\rho_{\text{fr}}(t)) = 1, \rho = |x|.$$

(24)

Here we will use another function which appears to work better in the case of spectral line shape which is a convolution of two essentially different line shapes (e.g., for Voigt line shape):

$$f_{\text{exact}}(0, t) = t\, G(\rho_{\text{fr}}(t)),$$

(25)

where

$$f_{exact}(0,t) = k_0^3 \frac{1}{(2\pi)^2} \int_{-\infty}^{\infty} P^2 [\exp\{t(J(P) - 1)\} - \exp\{-t\}] dP.$$

(26)

The relation between g and the exact solution of equation (1), f_{exact}, is described by the following equation:

$$Q_G(\rho, t) \equiv \frac{1}{\rho} G^{-1}\left(\frac{f_{\text{exact}}(\rho, t)}{t}\right),$$

(27)

where G^{-1} is the function reciprocal to the G function, $\rho \equiv k_0|\mathbf{r} - \mathbf{r}_0|$, k_0 is the absorption coefficient for photons at the frequency, corresponding to the line shape center,

$$Q_G\big(\rho, t(\rho, s)\big) \equiv Q_{G1}(s, \rho) = g(s),$$

(28)

$$Q_G(\rho(t, s), t) \equiv Q_{G2}(s, t) = g(s),$$

(29)

where the functions $t(\rho, s)$ and $\rho(t, s)$ are determined by the relation

$$s = \frac{\rho_{fr}(t)}{\rho}.$$

(30)

To prove the automodel solution one has to show weak dependence (independence) of Q_{G1} and Q_{G2} functions on, respectively, space coordinate and time. The results of the validation of the automodel solution and the reconstruction of function g from comparison of function (21) with computations of the Green's function for the Voigt and Holtsmark line shapes are given in what follows.

3.2. Automodel Solution for the Voigt Spectral Line Shape

The convolution of two line shapes with essentially different wings, exponential one, for the Doppler case, and power-law one, for the Lorentz case, makes the superdiffusive radiative transfer very sensitive to the contribution of the power-law wings of spectral line to the resulting long-tailed PDF. Numerical analysis shows that even a small admixture of the Lorentz line shape produces strong effect at large distances (for small values of p, respectively). It appears that for the Lorentz-dominated line shapes, i.e. moderate and large values of the Voigt parameter a, the

accuracy of automodel solution is high in almost the entire space of variables $\{\rho, t\}$, quite similar to the case [19, 26] of the superdiffusive transport for a 1D model PDF with the power-law wings. However, for a small a, the accuracy dramatically falls down in the essential part of the space of variables $\{\rho, t\}$. This failure stimulated searching for improving the accuracy by using the propagation front (25).

We illustrate the results of accuracy analysis with three figures. First, the functions $Q_{G2}(s,t)$ (29) are shown for different values of t in the range from $t_{min} = 30$ to $t_{max} = 10^6$. Further, the normalized functions $Q_{G2}(s,t)/\{Q_{G2}\}_{av}(s)$, where subscript av denotes averaging over time from $t_{min} = 30$ to $t_{max} = 10^8$, and the relative errors of the automodel solution $f_{auto}(\rho,t)/f_{exact}(\rho, t)$ are shown for the same range of time.

Distributed computations have been done on the cluster at NRC "Kurchatov Institute", http://ckp.nrcki.ru/ by means of the Everest, http://everest.distcomp.org/, a computing platform for publication, execution and composition of applications running across distributed computing resources [33]. A generic Everest application, the so-called Parameter Sweep, http://everest.distcomp.org/docs/ps, [34], was used to run a bunch of independent tasks at the cluster via special Everest-agent installed on the cluster.

The results of analysis for various values of the Voigt parameter a are shown in Figures 1 and 2.
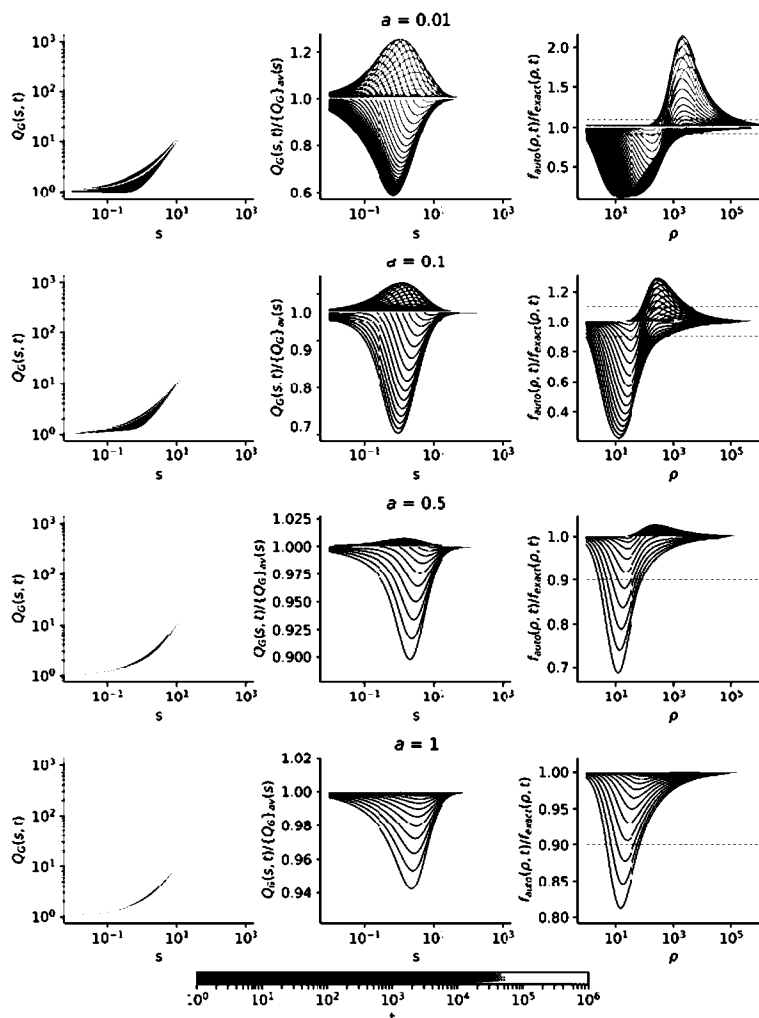

Figure 1. The result of accuracy analysis of automodel solution for various values of the Voigt parameter and the propagation front $\rho = \rho_{fr}$ taken in the form (25), for different values of t in the range from $t_{min} = 30$ to $t_{max} = 10^6$: (left) functions $Q_{G2}(s, t)$ (29); (center) normalized functions $Q_{G2}(s, t)/\{Q_{G2}\}_{av}(s)$, where subscript av denotes averaging over time from $t_{min} = 30$ to $t_{max} = 10^8$; (right) relative errors of the automodel solution $f_{auto}(\rho, t)/f_{exact}(\rho, t)$.
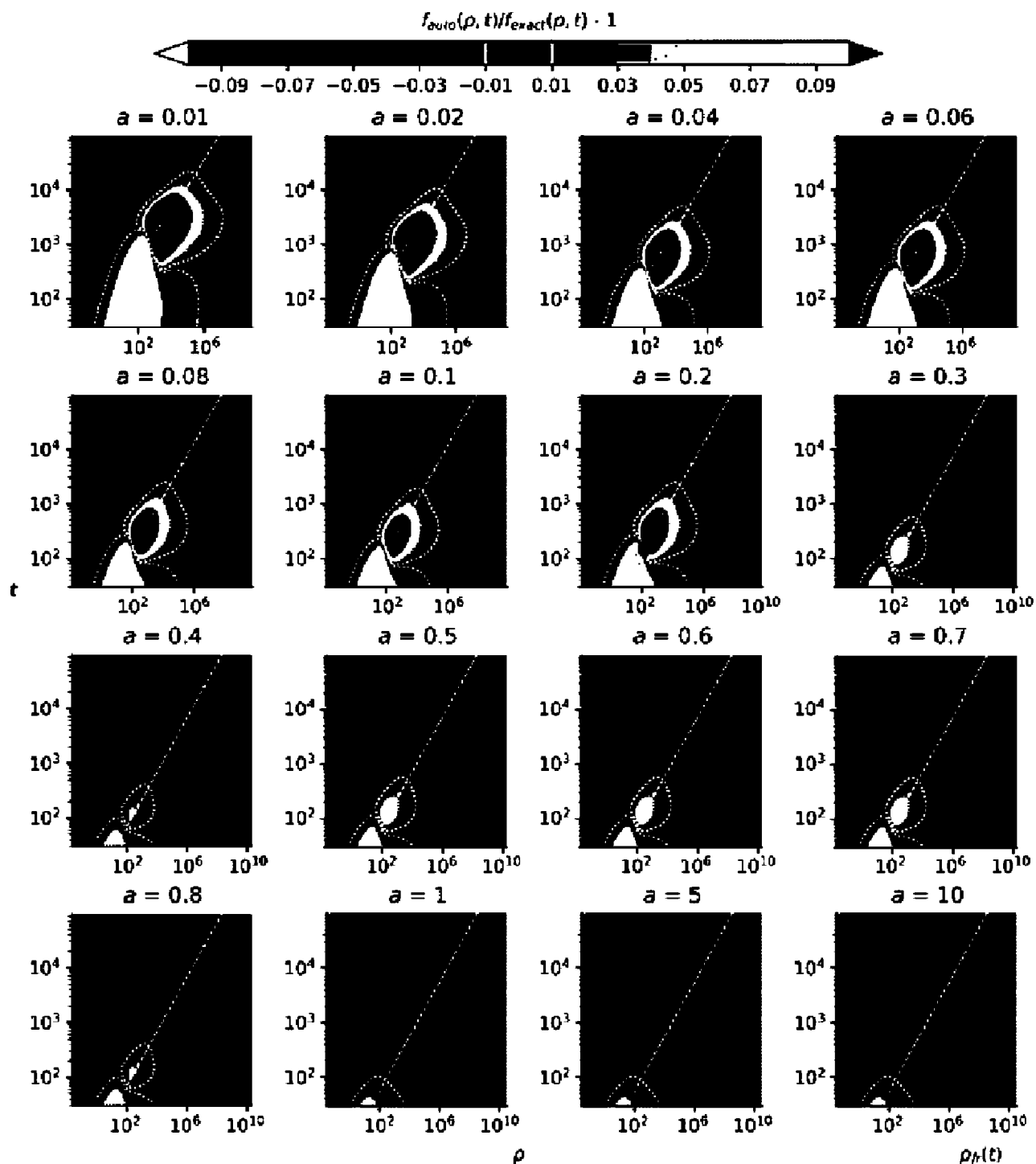
Figure 2. The level lines of the relative deviation of the automodel solution from the exact one, for the results from Figure 1.

3.3. Automodel solutiou for the Holtsmark spectral liue shape

Here we append the results [19, 25] of analyzing the automodel solution for the Holtsmark line shape with the results for the accuracy of automodel solution. Figure 3 shows the behavior of the automodel function Q_{G2} (29) and the relative deviation of the automodel solution from the exact one in the range from $t_{min} = 40$ to $t_{max} = 10^3$, with the time step equal to 20, for $40 \le t \le 500$, and 50, for $500 < t \le 1000$.
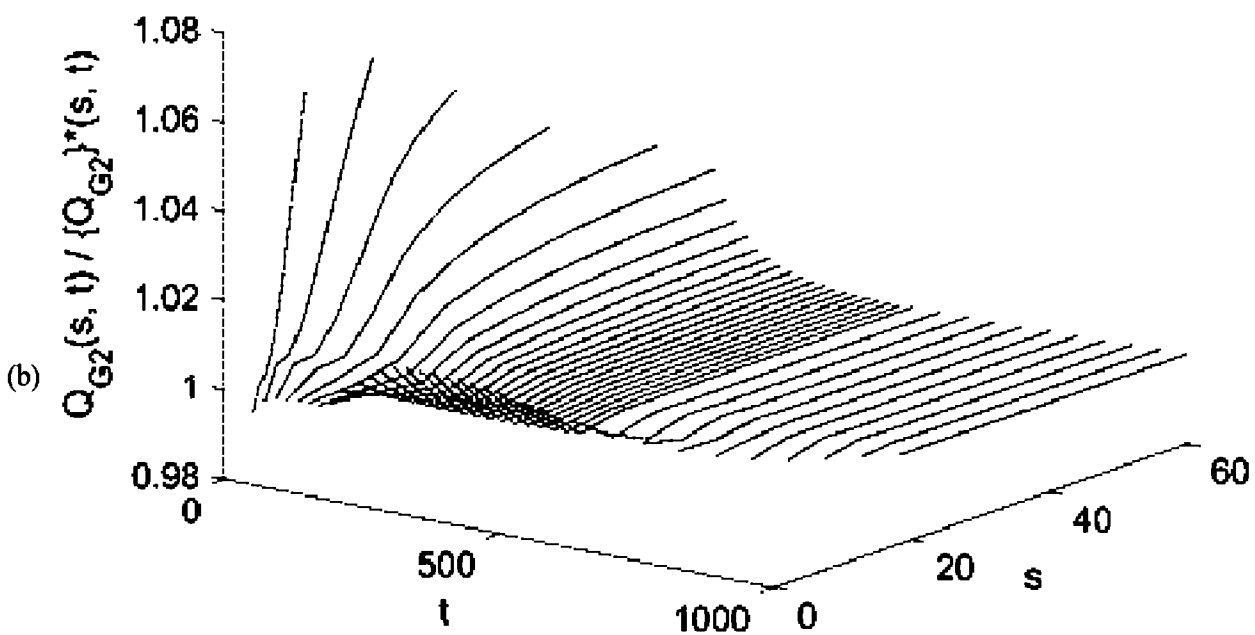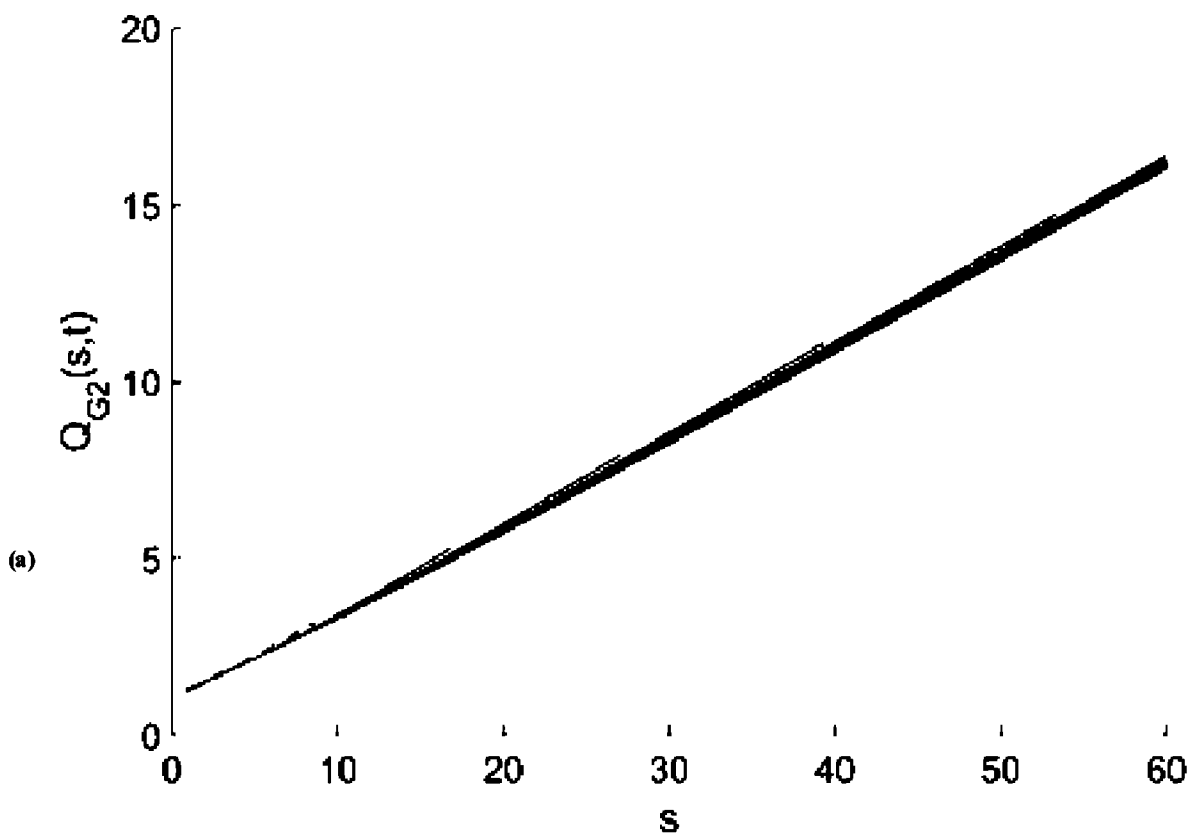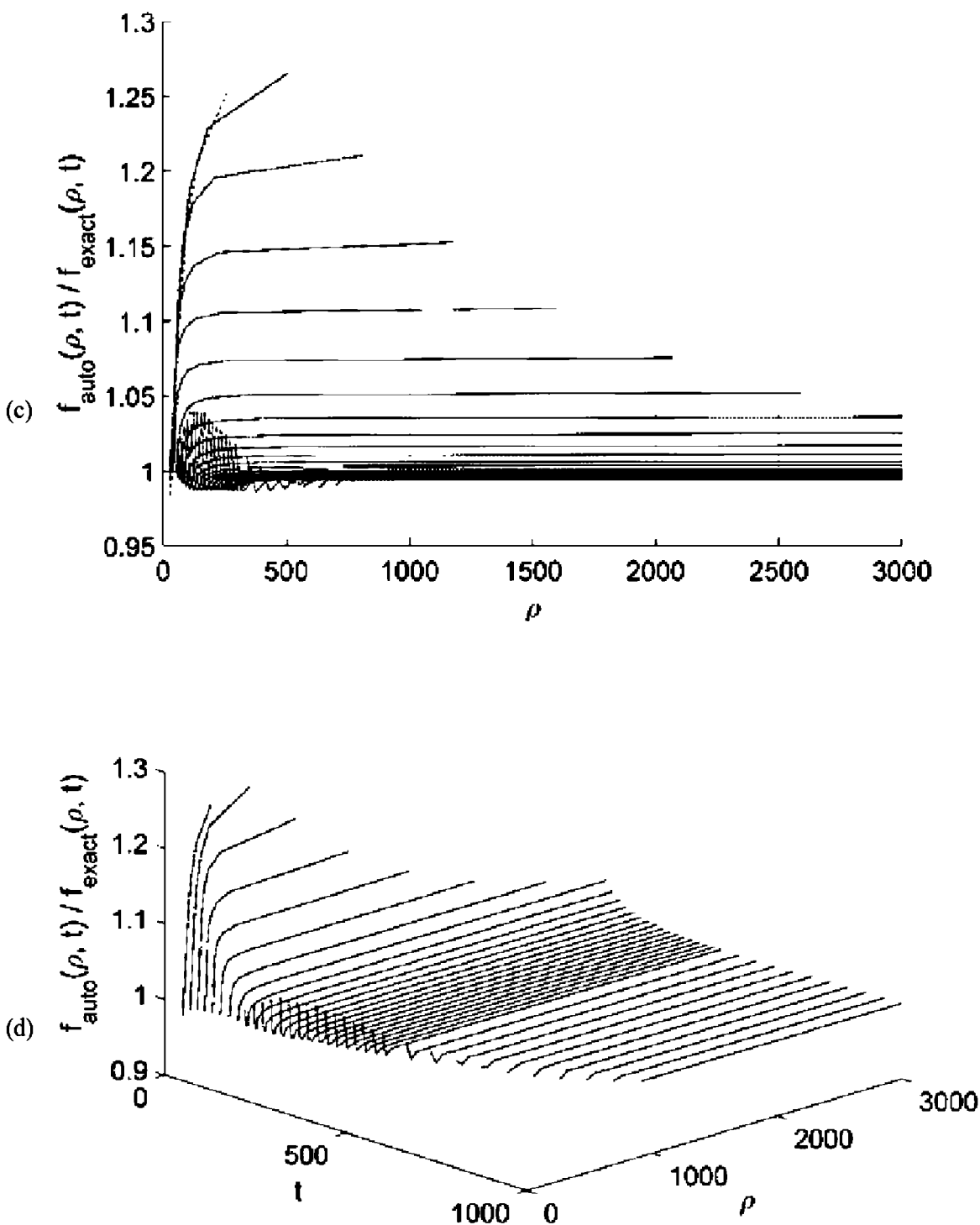
Figure 3. The result of accuracy analysis of automodel solution for the propagation front $\rho = \rho_{fr}$ taken in the form (24), for different values of t in the range from $t_{min} = 40$ (dashed line in (a) and (c) subplots and extreme left line in (b) and (d) subplots) to $t_{max} = 10^3$ (extreme right line in (b) and (d) subplots) with the time step equal to 20, if $40 \leq t \leq 500$, and 50; if $500 < t \leq 1000$: (a) functions $Q_{G2}(s,t)$ (29); (b) normalized functions $Q_{G2}(s,t)/\{Q_{G2}\}^*(s,t)$, where $\{Q_{G2}\}^*(s,t)$ is equal to $Q_{G2}(s,t = 160)$, for small s, and $Q_{G2}(s,t = 10^3)$, for large s; (c) relative error of the automodel solution $f_{auto}(\rho, t)/f_{exact}(\rho, t)$, (d) the same in the 3D view.

The results show that, similarly to the 1D transport for a model step-length PDF with power-law wings [19, 26], the accuracy of automodel solution is reasonably good for the propagation front (24).

4. CONCLUSIONS

The history of the research on the superdiffusive transport suggests that it is not possible to guess the "hidden" self-similarity from the general form of the transport equation, including the Biberman-Holstein equation, or from its analytical solutions in certain cases like the analytic solution [11] of the Biberman-Holstein equation. The approximate automodel (self-similar) solution [19] has been found thanks to:

- A hint from physics (namely, analysis of the kinetics of elementary excitation carriers),

- Interpolation of asymptotic solutions and solving an inverse problem which requires numerical simulations to verify the accuracy of automodel solution and determine the limits of its applicability.

Obtaining automodel (self-similar) solutions in the entire space of independent variables requires mass numerical simulations, however their total volume is significantly reduced due to self-similarity of the solution.

The Stark broadening of spectral lines, including the contribution of the impact Stark broadening to the Lorentz component of the Voigt line shape and the Holsmark broadening, produce the step-length probability distribution function (PDF) which makes the transport superdiffusive. The accuracy of approximate automodel solutions for the Green's function of the Biberman-Holstein equation for the Stark broadening of spectral lines is analyzed using the distributed computing. The high accuracy of automodel solutions in a wide range of parameters of the problem is shown. Massive computing experiments are done to verify automodel solutions. The Everest distributed computing platform and the cluster at NRC 'Kurchatov Institute' are used. The results, obtained with distributed computing, verified the high accuracy of automodel solutions in a wide range of space-time variables and enabled us to identify the limits of applicability of automodel solutions.

The sensitivity of the automodel solution to the definition of the front propagation scaling is shown for the line shape with two quite different line broadening mechanisms, and the improvement of the accuracy of automodel solution is achieved via generalization of the definition of the propagation front.

The present progress in describing the radiative transfer for infinite velocity of carriers, Eq. (1), may be extended to the case of a finite velocity [35, 36] (that includes the case of the resonance radiative transfer in astrophysics), where the exact solution and the asymptotics were also obtained [37].

References

[1] H.R. Griem, *Principles of Plasma Spectroscopy* (Cambridge University Press, Cambridge) 1997.

[2] I.I. Sobel'man, *Introduction to the Theory of Atomic Spectra* (Pergamon Press) 1972.

[3] V.I. Kogan; V.S. Lisitsa, G.V. Sholin, In *Reviews of Plasma Physics*; B.B. Kadomtsev, Ed., (Consultants Bureau, New York), 1987 13 261.

[4] V.S. Lisitsa, Usp. Fiz. Nauk **153** (1987) 379. English translation: Sov. Phys. Usp. **30** (1987) 927.

[5] L.A. Bureyeva, V.S. Lisitsa, *A Perturbed Atom*; (CRC Press LLC, Florida) 2000.

[6] E. Oks, *Stark Broadening of Hydrogen and Hydrogenlike Spectral Lines in Plasmas: The Physical Insight* (Alpha Science International, Oxford) 2006.

[7] E. Oks, *Diagnostics Of Laboratory And Astrophysical Plasmas Using Spectral Lines Of One-, Two-, and Three-Electron Systems* (World Scientific, New Jersey) 2017.

[8] A.V. Demura, Atoms **6** (2018) 33.

[9] L.M. Biberman, Zh. Eksper. i Teor. Fiz. **17** (1947) 416. English translation: Sov. Phys. JETP **19** (1949) 584.

[10] T. Holstein, Phys. Rev. **72** (1947) 1212.

[11] B.A. Veklenko, Zh. Eksper. i Teor. Fiz. **36** (1959) 204. English translation: Sov. Phys. JETP **9** (1959) 138.

[12] L.M. Biberman, V.S. Vorob'ev, I.T. Yakubov, *Kinetics of Nonequilibrium Low Temperature Plasmas* (Consultants Bureau, New York), 1987.

[13] V.A. Abramov, V.I. Kogan, V.S. Lisitsa, In *Reviews of Plasma Physics*, M.A. Leontovich, B.B. Kadomtsev, Eds. (New York, Consultants Bureau) 1987 **12** 151.

[14] A.N. Starostin, Resonance radiative transfer. *Encyclopedia of Low Temperature Plasma. Introduction Volume*, Fortov, V.E. Ed. (Nauka/Interperiodika, Moscow) 2000 **1** 471 [in Russian]. A.Yu. Sechin, A.N. Starostin, Yu.K. Zemtsov, D. I. Chekhov, A. G. Leonov, J. Quant. Spectroscopic. Radiat. Transfer **58** (1997) 887. A.E. Bulyshev, A.V. Demura, V.S. Lisitsa, A.N. Starostin, A.E. Suvorov, I.I. Yakunin, Sov. Phys.-JETP **81** (1995) 113.

[15] L.M. Biberman, Doklady Akademii nauk SSSR, Ser. Physics **49** (1948) 659 [in Russian].

[16] A.P. Napartovich, Teplofiz. Vys. Temp. **9** (1971) 26. English translation: High Temperature **9** (1971) 23.

[17] W. Kalkofen, In *Methods in Radiative Transfer*, W. Kalkofen, Ed. (Cambridge Univ. Press, Cambridge) 1984.

[18] G.B. Rybicki, Ibid., chapter 1.

[19] A.B. Kukushkin, P.A. Sdvizhenskii, J. Phys. A: Math. Theor. **49** (2016) 255002.

[20] M. Shlesinger, G.M.Zaslavsky, U. Frisch, Eds. *Lévy Flights and Related Topics in Physics* (Springer-Verlag, Berlin) 1995.

[21] B.B. Mandelbrot, *The Fractal Geometry of Nature* (W. H. Freeman, New York), 1982.

[22] I.I. Eliazar, M. F. Shlesinger, Phys. Rep. **527** (2013) 101.

[23] A.A. Dubkov, B. Spagnolo, V.V. Uchaikin, Int. J. Bifurcation Chaos **18** (2008) 2649.

[24] J. Klafter, I.M. Sokolov, Physics world **18** (2005) 29.

[25] A.B. Kukushkin, P.A. Sdvizhenskii, J. Phys. Conf. Series **941** (2017) 012050.

[26] A.B. Kukushkin, V.S. Neverov, P.A. Sdvizhenskii, V.V. Voloshinov, International Journal of Open Information Technologies (INJOIT) **6** (2018) 38.

[27] V.I. Kogan, In *A Survey of Phenomena in Ionized Gases (Invited Papers)* [in Russian], (Proc. ICPIG'67), Vienna: IAEA, 1968, 583. V.I. Kogan, In *Encyclopedia of Low Temperature Plasma. Introduction Volume*, V.E. Fortov, Ed. (Nauka/Interperiodika, Moscow) 2000 **1** 481 [in Russian].

[28] Y.Y. Abramov, A.P. Napartovich, Astrofizika **5** (1969) 187 [in Russian].

[29] A.B. Kukushkin, P.A. Sdvizhenskii, 2014 Proceedings of 41st EPS Conference on Plasma Physics, Berlin, Germany, 23 – 27 June 2014, ECA, 38F, P4.133.

[30] A.B. Kukushkin, P.A. Sdvizhenskii, V.V. Voloshinov, A.S. Tarasov, International Review of Atomic and Molecular Physics (IRAMP) **6** (2015) 31.

[31] S.E. Frish, *Optical Spectra of Atoms* (Fizmatgiz, Moscow-Leningrad) 1963 [in Russian].

[32] I.S. Gradshtein,; I. M. Ryzhik, *Tables of integrals, sums, series and products* (Fizmatgiz, Moscow) 1963 [in Russian].

[33] O. Sukhoroslov, S. Volkov, A. Afanasiev, In 14th International Symposium on Parallel and Distributed Computing (ISPDC), Limassol, Cyprus, 29 June-2 July 2015, *IEEE*, **2015**, 175.

[34] S. Volkov, O. Sukhoroslov, Procedia Computer Science **66** (2015) 477.

[35] V. Zaburdaev, S. Denisov, J. Klafter, Reviews of Modern Physics **87** (2015) 483.

[36] V.Yu. Zaburdaev, K.V. Chukbar, JETP **94** (2002) 252.

[37] A.A. Kulichenko, A.B. Kukushkin, International Review of Atomic and Molecular Physics (IRAMP) **8** (2017) 5.